2013 IEEE/RSJ International Conference on
Intelligent Robots and Systems (IROS)
November 3-7, 2013. Tokyo, Japan

# Kinodynamic Motion Planning and Control for an X4-Flyer Using Anisotropic Damping Forces

Kimiko Motonaka[1], Keigo Watanabe[1] and Shoichi Maeyama[1]

*Abstract*— **We present a novel method to control an X4-Flyer using kinodynamic motion planning. Kinodynamic motion planning is the planning technique of generating a control input by solving the problems of kinematic constraints and dynamic constraints simultaneously, and it is useful for simpler generation of the control input. In this paper, we extend existing kinodynamic motion planning, which uses "Harmonic potential field (HPF)" and some damping forces for the control of simple point mass, to the motion planning for an X4-Flyer, which is a complex multivariable system. Then, we use "nonlinear anisotropic damping forces (NADFs)," which is proposed by Masoud, as damping force. In the simulation, a method using NADFs is compared with that using viscous damping forces. From the simulation, it is confirmed that the kinodynamic motion planning can be realized for an X4-Flyer.**

## I. Introduction

Motion planning is a very critical factor for an autonomous mobile robot. There are two important constraints, when a robot is controlled in a real environment. One is kinematic constraints, which is influenced from robot configuration, position and velocity. By solving kinematic constraints, ideal behavior is calculated because the robot mass or acceleration is not considered in kinematic constraints. The other is dynamic constraints, which is influenced from robot acceleration and forces. By solving the dynamic constraints, actual behavior in a real environment can be calculated because the inertial force or acceleration of the robot is considered in dynamic constraints. In conventional motion planning, dynamic constraints are generally solved by designing control input according to the result of kinematic constraints, after solving kinematic constraints by using path planning[1]–[3].

There is "kinodynamic motion planning" that is aimed at solving these two constraints simultaneously, for designing the control input from the current state[4]. Kinodynamic motion planning can design the control input in one-step, and therefore it has an advantage of being able to decide the control input simply, compared to existing motion planning[5]–[7]. There are many techniques for kinodynamic motion planning, and kinodynamic motion planning based on using "Harmonic potential field (HPF)" was proposed as one of them. An HPF is a smooth potential field which has no stationary points[8]. By using its gradient vector, it is guaranteed that a kinematic trajectory can reliably reach a target point from anywhere in the field while avoiding obstacles[9]–[11]. When using an HPF in kinodynamic motion planning, viscous damping forces are generally added to the control input together with the gradient of the HPF to prevent a deviation from the gradient vector. However, the method assumes that the controlled object moves slowly by decelerating. So, Masoud proposed the "Nonlinear anisotropic damping forces (NADFs)" as an alternative to viscous damping forces[12]. The NADFs can consider the direction of the gradient vector, and NADFs decelerate the controlled object only when the controlled object deviates from the gradient vector. Masoud also proposed "clamping control" for suppressing an overshoot or oscillation. In the simulation of point mass control, it was confirmed that the kinodynamic motion planning using NADFs and "clamping control" can guide the point mass to the target point quickly[12][13].

This method tested its usefulness in point mass control simulations only. In this paper, we use an X4-Flyer as a more realistic controlled object. An X4-Flyer is a vertical takeoff and landing (VTOL) aerial robot with four rotors, and it has received attention in recent years as search and rescue robots because of its highly maneuverability and hovering ability. Actually, there are recently many researches [14]–[16] on the autonomous locomotion for an X4-Flyer. Autonomous locomotion of an X4-Flyer may become easier by extending the kinodynamic motion planning to the control of an X4-Flyer.

In this paper, we show that the kinodynamic motion planning can also be applied to an X4-Flyer, though it was limited to a point mass in previous researches. Especially, it is confirmed that the kinodynamic motion planning using NADFs is useful for the motion planning of an X4-Flyer, compared to one using only viscous damping forces.

## II. Kinodynamic Motion Planning Using an HPF

This research is aimed at extending kinodynamic motion planning using NADFs and HPF to the X4-Flyer. First of all, the concept of kinodynamic motion planning is clarified. In the case where an object having a mass is controlled, the design needs to consider dynamic constraints of the controlled object. In motion planning, the control input is generally designed by solving dynamic constraints, after solving kinematic constraints. By contrast, kinodynamic motion planning can design the control input easily from the robot states by solving kinematic constraints and dynamic constraints simultaneously. In this section, conventional kinodynamic motion planning for a point mass and HPF used in existing methods are overviewed.

[1]K. Motonaka, K. Watanabe and S. Maeyama are with the Graduate School of Natural Science and Technology, Okayama University, Okayama, Japan k.motonaka at usm.sys.okayama-u.ac.jp

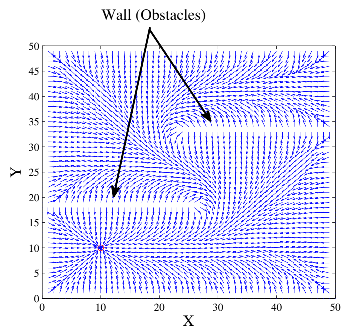


Fig. 1: Normalized gradient field

### A. Harmonic Potential Field

There is an HPF as a tool for realizing kinodynamic motion planning. The HPF is a smooth potential field that has no stationary points. The gradient of the HPF is generated by repulsive forces from the obstacles and attractive forces form the target point. It is guaranteed that a kinematic trajectory, which is generated by using the gradient of the HPF, can reliably reach a target point. By adding the gradient to the control input, it can decide the control input that can guide the controlled object from the current position to the target point while avoiding obstacles.

Figure 1 shows gradient vectors calculated from an HPF. Note that these vectors have been normalized by the grid size. The position circled in Fig. 1 shows the configured target point. It is confirmed that a kinematic trajectory using the gradient of HPF can reach a target point from anywhere in the field while avoiding obstacles.

### B. Kinodynamic Motion Planning for a Point Mass

If the gradient of HPF is directly used for the control input for a point mass, the point mass is accelerated unlimitedly and goes out of control. Then, Rimon and Koditschek [6] proposed to use viscous damping forces for kinodynamic motion planning using HPF. By using viscous damping forces, a control input suppresses any acceleration consistently, and the controlled object can be stabilized. However, there are disadvantages that it takes much time to reach a target point because such a method keeps the velocity of the controlled object low at anywhere. Masoud and Masoud proposed nonlinear anisotropic damping forces, NADFs, to compensate for this disadvantage[17]. However, when using this method, the controlled object cannot keep its state at the target point, and it oscillates and/or diverges. Therefore, Masoud also proposed to use "clamping control" at around the target point. By applying the clamping control, the controlled object is attracted to the target point and converged. In this section, when using viscous damping forces, NADFs and clamping control, the control input of kinodynamic motion planning is described.

*1) Using viscous damping forces:* When controlling a point mass with 1 kg, the control input $\boldsymbol{u}$ based on kinodynamic motion planning using viscous damping forces is given as follow:

$$\boldsymbol{u} = -b\dot{\boldsymbol{x}} - \nabla V(\boldsymbol{x}) \tag{1}$$

where $b$ denotes a damping coefficient and also is positive constant. In Eq. (1), the control input $\boldsymbol{u}$ consists of the gradient of the current position, $-\nabla V$, and the damping force linearly proportional to the velocity, $-b\dot{\boldsymbol{x}}$. This damping force increases in proportion to increasing of the damping coefficient or velocity, and suppresses the acceleration of a point mass.

*2) Using NADFs:* The method described above, which is based on HPF and viscous damping forces, has disadvantages that it takes much time to reach a target point. Masoud [12] proposed a control method that can cancel out the unnecessary direction forces by combining the gradient of HPF with NADFs. The following equation is the controller proposed by Masoud[12]:

$$\boldsymbol{u} = -b_d \cdot h(\boldsymbol{x}, \dot{\boldsymbol{x}}) - k \cdot \nabla V(\boldsymbol{x}) \tag{2}$$

where $b_d$ and $k$ denote positive constant gains, and $h(\boldsymbol{x}, \dot{\boldsymbol{x}})$ is the proposed NADFs, which is given by

$$\begin{aligned} & h(\boldsymbol{x}, \dot{\boldsymbol{x}}) \\ = \ & \left[\mathbf{n}^{\mathrm{T}}\dot{\boldsymbol{x}}\mathbf{n} + \left(\frac{V(\boldsymbol{x})^{\mathrm{T}}}{\|\nabla V(\boldsymbol{x})\|} \cdot \dot{\boldsymbol{x}} \cdot \Phi(\nabla V(\boldsymbol{x})^{\mathrm{T}}\dot{\boldsymbol{x}})\right)\frac{V(\boldsymbol{x})^{\mathrm{T}}}{\|\nabla V(\boldsymbol{x})\|}\right] \end{aligned} \tag{3}$$

Here, $\mathbf{n}$ is a unit vector orthogonal to $\nabla V$ and $\Phi$ is the unit step function. The function $\Phi$ takes 0 if $\nabla V(\boldsymbol{x})^{\mathrm{T}}\dot{\boldsymbol{x}}$ is negative, and otherwise takes 1. The function is prepared to check the consistency between the direction of current velocity of the controlled object and the direction of gradient of HPF. If the direction of the current velocity matches the gradient direction, then the unit step function takes 1, thus, a force toward the current velocity direction is increased. By contrast, if their directions are not matched, then the unit step function takes 0, thus, a force canceling the current velocity is added. At the same time, a force toward the gradient direction is added, and the controlled object is returned to the kinematic trajectory. As described above, the NADFs can guide the controlled object in less time compared with the case using viscous damping forces, because NADFs consider the direction of current velocity and gradient of HPF, and prevent unnecessary deceleration.

*3) Using NADFs and clamping control:* The control using NADFs can guide a controlled object to a target point while canceling external forces. However, after reaching to the target point, the controlled object sometimes cannot maintain any states and therefore it oscillates and/or diverges. Therefore, we apply "clamping control." By applying such clamping control, the controlled object is attracted to the target point and converged. Fig. 2 shows the schematic structure of the clamping control. The clamping control is applied in a circle area as shown in Fig. 2. The center point of the region is a target point and its radius is $\sigma$. In this area, if a controlled object moves toward the target point, then the clamping control is not applied. By contrast, if a controlled object moves against the target point in the area,

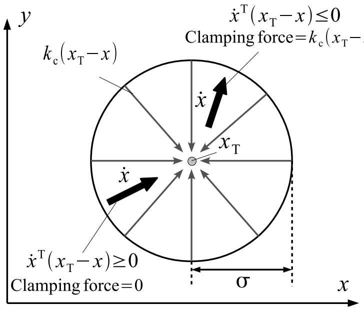


Fig. 2: The clamping control

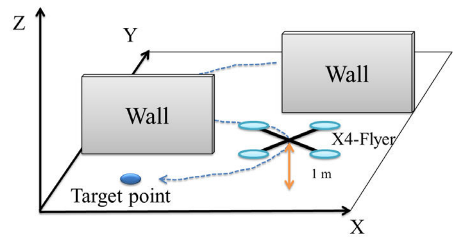


Fig. 3: Example behavior of an X4-Flyer

then the clamping control adds a force $(\boldsymbol{x}-\boldsymbol{x}_{\mathrm{T}})$ in a direction toward the target point, and converges a controlled object on the target point. Appending the clamping control to the control input based on NADFs given in Eq. (2), it follows that

$$\boldsymbol{u} = -b_d \cdot h(\boldsymbol{x}, \dot{\boldsymbol{x}}) - k \cdot \nabla V(\boldsymbol{x}) - k_{\mathrm{c}} \cdot \boldsymbol{F}_{\mathrm{C}}(\boldsymbol{x}, \dot{\boldsymbol{x}}) \quad (4)$$

where $k_c$ denotes a positive constant gain related to the clamping control and $F_C$ is given by

$$\boldsymbol{F}_{\mathrm{C}}(\boldsymbol{x}, \dot{\boldsymbol{x}}) = (\boldsymbol{x}_{\mathrm{T}} - \boldsymbol{x}) \cdot \Phi(\sigma - |\boldsymbol{x}_{\mathrm{T}} - \boldsymbol{x}|) \cdot \Phi(\dot{\boldsymbol{x}}^{\mathrm{T}}(\boldsymbol{x}_{\mathrm{T}} - \boldsymbol{x})) \quad (5)$$

Here, the unit step function $\Phi(\sigma - |\boldsymbol{x}_{\mathrm{T}} - \boldsymbol{x}|)$ is set to check whether the controlled object is in the region, and $\Phi(\dot{\boldsymbol{x}}^{\mathrm{T}}(\boldsymbol{x}_{\mathrm{T}} - \boldsymbol{x}))$ is prepared to check whether the direction of current velocity of the controlled object consists with the direction of the target point. By checking these two conditions, the clamping control is added only when needed.

## III. Proposed Kinodynamic Motion Planning for an X4-Flyer

### A. Dynamic Model of an X4-Flyer

In the previous section, conventional kinodynamic motion planning for a point mass was described. In this section, to extend the kinodynamic motion planning to more realistic problem, we apply the kinodynamic motion planning to the control of an X4-Flyer, which is vertical takeoff and landing (VTOL) aerial robot. The X4-Flyer can be controlled by applying nonholonomic control[18]. In that case, one position and three attitude angles in the position $(x, y, z)$ and the attitude $(\phi, \theta, \psi)$ of the X4-Flyer can be controlled. In this paper, it is assumed that the X4-Flyer flies while keeping its elevation $z$, and kinodynamic motion planning based on using HPF is applied, which is generated on X-Y plane (see Fig. 3). Therefore, kinodynamic motion planning is realized by combining an input based on nonholonomic control $\boldsymbol{u}_c$, which is for keeping its attitude (elevation $z$ and an attitude $(\phi, \theta, \psi)$), and an input based on kinodynamic control $\Delta\boldsymbol{u}$ for moving on X-Y plane. Thus, the system input $\boldsymbol{U} = [U_1\ U_2\ U_3\ U_4]^{\mathrm{T}}$ is as follows:

$$\boldsymbol{U} = \boldsymbol{u}_c + \Delta\boldsymbol{u} \quad (6)$$

Here, $U_1$ is a control input for acting on each translational motion, and $U_2$, $U_3$ and $U_4$ are control inputs for acting on roll angle $\phi$, pitch angle $\theta$ and yaw angle $\psi$ respectively. In the following subsections, we describe the dynamic model of an X4-Flyer, the control input based on nonholonomic control $\boldsymbol{u}_c$ and the proposed control input based on kinodynamic motion planning $\Delta\boldsymbol{u}$.

An X4-Flyer controls its three directional positions $(x, y, z)$, (which moves back-and-forth, right-and-left and up-and-down), and three attitude angles $(\phi, \theta, \psi)$, (which performs roll, pitch and yaw motion), by using mounted 4 rotors on the airframe. Figure 4 shows the model of the X4-Flyer, where B means a body coordinate system and E means the world coordinate system. Assume that the positive rotation angle $(\phi, \theta, \psi)$ is directed clockwise when we see the corresponding coordinate axis $(x, y, z)$ from the negative to the positive direction. Mounted rotors (rotor 1 to rotor 4) turn in arrows direction in Fig. 4 respectively. Z-directional motion is controlled by increasing/decreasing the four rotors' speed together. Roll direction motion is controlled by changing the rotor 2 and rotor 4's speed while keeping rotor 1 and rotor 3's speed constant. Pitch direction motion is controlled by changing the rotor 1 and rotor 3's speed while keeping rotor 2 and rotor 4's speed constant. Yaw direction motion is controlled by increasing/decreasing the rotor 2 and rotor 4's speed, and decreasing/increasing rotor 1 and rotor 3's speed simultaneously.

Let define $m$ [kg] as the mass of the X4-Flyer, $l$ [m] as the length from the center of airframe to the center of rotor, $g$ [m/s$^2$] as the gravity acceleration, $I_x$, $I_y$ and $I_z$ [kg/m$^2$] as the inertial moment around each axis respectively, and $J_r$ [kg/m$^2$] as the inertial moment of a rotor. Here, $U_1$ is the control input for acting on each translational motion, and $U_2$, $U_3$ and $U_4$ are the control inputs for acting on roll motion, pitch motion and yaw motion respectively. The dynamic model of the X4-Flyer is:

$$\begin{cases} \ddot{x} &= (\cos\phi\sin\theta\cos\psi + \sin\phi\sin\psi)\frac{1}{m}U_1 \\ \ddot{y} &= (\cos\phi\sin\theta\sin\psi + \sin\phi\cos\psi)\frac{1}{m}U_1 \\ \ddot{z} &= -g + (\cos\phi\cos\theta)\frac{1}{m}U_1 \\ \ddot{\phi} &= \dot{\theta}\dot{\psi}(\frac{I_y - I_z}{I_x}) - \frac{J_r}{I_x}\dot{\theta}\Omega + \frac{l}{I_x}U_2 \\ \ddot{\theta} &= \dot{\phi}\dot{\psi}(\frac{I_z - I_x}{I_y}) - \frac{J_r}{I_y}\dot{\phi}\Omega + \frac{l}{I_y}U_3 \\ \ddot{\phi} &= \dot{\phi}\dot{\theta}(\frac{I_x - I_y}{I_z}) + \frac{1}{I_z}U_4 \end{cases} \quad (7)$$

Then, $\Omega$ and the system's inputs $U_1$, $U_2$, $U_3$, $U_4$ can be written by using the rotational speed $\omega_i$ of the rotor $i$

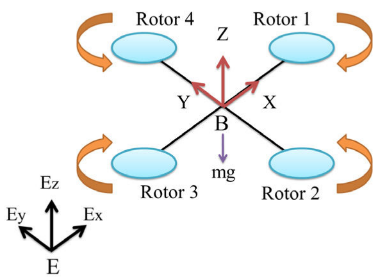


Fig. 4: Structure of the X4-Flyer and the definition of coordinates

($i$=1,...,4), i.e.,

$$\begin{cases} U_1 &= b(\omega_1^2+\omega_2^2+\omega_3^2+\omega_4^2) \\ U_2 &= b(\omega_4^2-\omega_2^2) \\ U_3 &= b(\omega_3^2-\omega_1^2) \\ U_4 &= d(\omega_2^2+\omega_4^2-\omega_1^2-\omega_3^2) \\ \Omega &= \omega_2+\omega_4-\omega_1-\omega_3 \end{cases} \quad (8)$$

Here $b$ is the thrust coefficient and $d$ is the drag coefficient.

### B. Nonholonomic Control Input for the X4-Flyer

The X4-Flyer has constraints between the angle of roll/pitch and y/x axis direction. These constraints can be shown in equation by using dynamic model of the X4-Flyer:

$$\begin{array}{l} \ddot{x}\cos\psi + \ddot{y}\sin\psi + \tan\theta(g-\ddot{z}) = 0 \\ \ddot{x}\sin\psi - \ddot{y}\cos\psi + \sin\phi\sqrt{\ddot{x}^2+\ddot{y}+(\ddot{z}-g)^2} = 0 \end{array} \quad (9)$$

Nonholonomic control can be applied to the X4-Flyer based on these two constraints. By applying nonholonomic control, one position and three attitude angles can be controlled out of the position $(x, y, z)$ and attitude angle $(\phi, \theta, \psi)$ of the X4-Flyer.

Then, the control input $\boldsymbol{u}_\mathrm{c} = [u_{c1}\ u_{c2}\ u_{c3}\ u_{c4}\ ]^\mathrm{T}$ for z direction and three attitude angle are

$$\begin{cases} u_{c1} = \frac{mg}{\cos\phi\cos\theta} - \frac{m\hat{U}_1}{\cos\phi\cos\theta} \\ u_{c2} = -\frac{I_x}{l}(\phi-\phi_\mathrm{T}) - k_1\dot{\phi} \\ u_{c3} = -\frac{I_y}{l}(\theta-\theta_\mathrm{T}) - k_2\dot{\theta} \\ u_{c4} = -I_z(\psi-\psi_\mathrm{T}) - k_3\dot{\psi} \end{cases} \quad (10)$$

where $\hat{U}_1$ is

$$\hat{U}_1 = k_4(z-z_\mathrm{T}) + k_5\dot{z} \quad (11)$$

Here, $k_1 \sim k_5$ are positive constant gains, and $z_\mathrm{T}$ is a desired altitude and $(\phi_\mathrm{T}, \theta_\mathrm{T}, \psi_\mathrm{T})$ are the desired angles. By using this control input based on nonholonomic control, the X4-Flyer can keep its altitude and angles.

### C. Proposed Kinodynamic Motion Planning for the X4-Flyer

In this subsection, an existing control input for a point mass is extended to the control input $\boldsymbol{u} = \boldsymbol{u}_c + \Delta\boldsymbol{u}$, which can be applied to the X4-Flyer. Here, $\boldsymbol{u}_c$ is the control input based on nonholonomic control, and $\Delta\boldsymbol{u} = [\Delta u_1\ \ \Delta u_2\ \ \Delta u_3\ \ \Delta u_4]$ is the control input based on the kinodynamic motion planning. In this paper, it is assumed that the X4-Flyer moves on X-Y plane while hovering constant altitude. Then, X-Y directional control is achieved by applying the gradient of HPF in X-Y plane and each damping forces to the control input for roll angle $\phi$ and pitch angle $\theta$ as the kinodynamic control input $\Delta\boldsymbol{u}$. Three types of control input based on the kinodynamic motion planning are discussed below.

*1) Using viscous damping forces:* For the control of the X4-Flyer, the control input $\Delta\boldsymbol{u}$ based on the kinodynamic motion planning using viscous damping forces can be extended as

$$\Delta\boldsymbol{u} = -b_\mathrm{c}\cdot\dot{\boldsymbol{x}} - k_v\nabla V(\boldsymbol{x}) \quad (12)$$

Here, $b_\mathrm{c}$ and $k_v$ are positive constant gains, $\dot{\boldsymbol{x}} = [0\ \dot{y}\ \dot{x}\ 0]^\mathrm{T}$, and $\nabla V(\boldsymbol{x}) = [0\ f_y\ f_x\ 0]^\mathrm{T}$. Note that, $f_x$ and $f_y$ mean the gradient of HPF parallel to the direction of x- and y-axis respectively.

*2) Using NADFs:* The control input $\Delta\boldsymbol{u}$ based on the kinodynamic motion planning using NADFs can be extended as

$$\Delta\boldsymbol{u} = -b_d\cdot\boldsymbol{h}(\boldsymbol{x},\dot{\boldsymbol{x}}) - k_v\nabla V(\boldsymbol{x}) \quad (13)$$

Here, $b_d$ is a positive constant gain, $\boldsymbol{h}(\boldsymbol{x},\dot{\boldsymbol{x}}) = [0\ h(y,\dot{y})\ h(x,\dot{x})\ 0]^\mathrm{T}$, and $\nabla V(\boldsymbol{x}) = [0\ f_y\ f_x\ 0]^\mathrm{T}$.

*3) Using NADFs and clamping control:* The control input $\Delta\boldsymbol{u}$ based on the kinodynamic motion planning using NADFs and clamping control can be extended as

$$\Delta\boldsymbol{u} = \begin{cases} -b_c\cdot\dot{\boldsymbol{x}} - k_v\nabla V(\boldsymbol{x}) - k_c\cdot\boldsymbol{F}_\mathrm{C}(\boldsymbol{x},\dot{\boldsymbol{x}}) \\ \qquad \text{if} \quad \sigma < \sqrt{(x-x_\mathrm{T})^2+(y-y_\mathrm{T})^2} \\ -b_d\cdot\boldsymbol{h}(\boldsymbol{x},\dot{\boldsymbol{x}}) - k_v\nabla V(\boldsymbol{x}) \\ \qquad \text{otherwise} \end{cases} \quad (14)$$

Here, $\sigma$ is a radius of region, in which clamping control is applied, $x_\mathrm{T}$ and $y_\mathrm{T}$ are the x-y coordinate of a target point, $b_\mathrm{c}$ and $k_\mathrm{c}$ are the positive constant gains, and $\boldsymbol{F}_\mathrm{C}(\boldsymbol{x},\dot{\boldsymbol{x}}) = [0\ \ F_\mathrm{C}(y,\dot{y})\ \ F_\mathrm{C}(x,\dot{x})\ \ 0]^\mathrm{T}$. In around of the target point, it is advisable to decelerate constantly for avoiding sudden braking. Therefore, not only clamping control is applied but also the control is switched from using NADFs to the control using viscous damping forces in around of the target point.

## IV. Simulations

In this section, we conduct some simulations for comparing three methods as described above (using viscous damping forces, using NADFs, and combining NADFs and clamping control) by checking the behavior of the X4-Flyer.

### A. Conditions

The initial states in X-Y plane in an assumed environment are shown in Fig. 5, where there are two walls as obstacles in the environment. The S-shaped curve trajectory drawn in Fig. 5 is a kinematic trajectory calculated from the gradient of HPF. In this simulation, it is assumed that the X4-Flyer moves from the initial position $(x_0, y_0, z_0) = (40, 40, 1)$ to the target position $(x_\mathrm{T}, y_\mathrm{T}, z_\mathrm{T}) = (10, 10, 1)$ while keeping its altitude $z = 1$ [m]. The initial attitude is set to $(\phi, \theta, \psi) = (0, 0, 0)$, and the target attitude is set to $(\phi_\mathrm{T}, \theta_\mathrm{T}, \psi_\mathrm{T}) = (0, 0, 0)$. The model of the X4-Flyer that is developed in our

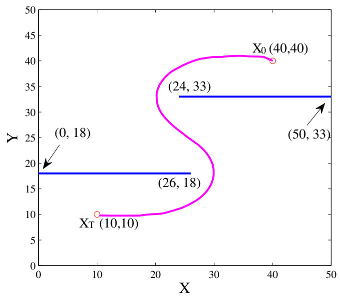


Fig. 5: Simulation environment

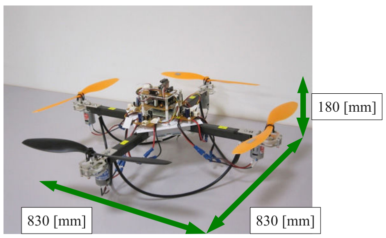


Fig. 6: The X4-Flyer

laboratory shown in Fig. 6 is used for the controlled X4-Flyer in simulations. Table I shows each parameter for simulations. Thrust coefficient $b$ and drag coefficient $d$ were calculated from preliminary experiments using the actual equipment. Then, the behavior of the X4-Flyer is compared when giving three kinds of control input below:

$$\boldsymbol{U} = \boldsymbol{u}_c - b_c \cdot \dot{\boldsymbol{x}} - k_v \nabla V(\boldsymbol{x}) \tag{15}$$

$$\boldsymbol{U} = \boldsymbol{u}_c - b_d \cdot \boldsymbol{h}(\boldsymbol{x}, \dot{\boldsymbol{x}}) - k_v \nabla V(\boldsymbol{x}) \tag{16}$$

$$\boldsymbol{U} = \begin{cases} \boldsymbol{u}_c - b_c \cdot \dot{\boldsymbol{x}} - k_v \nabla V(\boldsymbol{x}) - k_c \cdot \boldsymbol{F}_C(\boldsymbol{x}, \dot{\boldsymbol{x}}) \\ \qquad \text{if } \sigma < \sqrt{(x - x_T)^2 + (y - y_T)^2} \\ \boldsymbol{u}_c - b_d \cdot \boldsymbol{h}(\boldsymbol{x}, \dot{\boldsymbol{x}}) - k_v \nabla V(\boldsymbol{x}) \\ \qquad \text{otherwise} \end{cases} \tag{17}$$

where Eqs. (15), (16) and (17) are control inputs for the cases when applying viscous damping forces, NADFs, and NADFs plus clamping control respectively. Each gain is decided from empirical rules and set as shown in Table II.

TABLE I: Model parameters for the X4-Flyer

| Parameter | Description | Value | Unit |
|---|---|---|---|
| $g$ | Gravity | 9.80665 | m/s$^2$ |
| $m$ | Mass | 1.3 | kg |
| $l$ | Distance | 0.248 | m |
| $I_x$ | Roll inertia | 0.01467 | kg·m$^2$ |
| $I_y$ | Pitch inertia | 0.01467 | kg·m$^2$ |
| $I_z$ | Yaw inertia | 0.02331 | kg·m$^2$ |
| $J_r$ | Rotor inertia | 175.69×10$^{-6}$ | kg·m$^2$ |
| $b$ | Thrust factor | 0.0000434 | |
| $d$ | Drag factor | 0.000002188 | |

TABLE II: Control gains for the X4-Flyer

| Gain | Value | Gain | Value |
|---|---|---|---|
| $k_1$ | 0.015 | $k_2$ | 0.015 |
| $k_3$ | 0.007 | $k_4$ | 10.0 |
| $k_5$ | 25.0 | $k_v$ | 0.001 |
| $b$ | 0.002 | $b_d$ | 0.002 |
| $b_c$ | 0.004 | $\sigma$ | 10 |

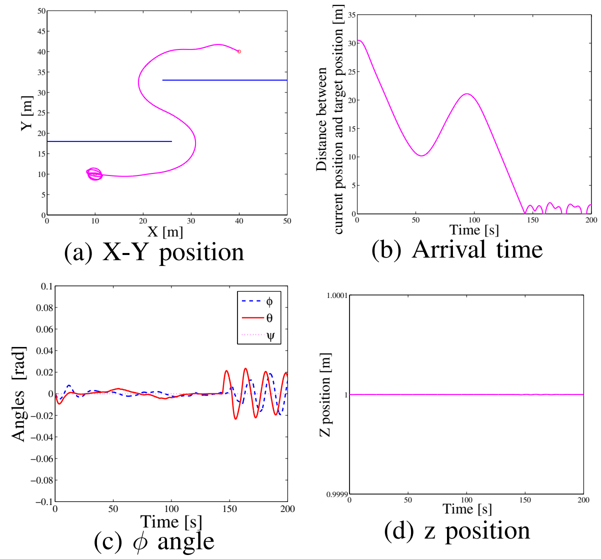


(a) X-Y position (b) Arrival time (c) $\phi$ angle (d) z position

Fig. 7: Results with viscous damping forces

## B. Results

Fig. 7 is the graph of trajectory of (a) X-Y position, (b) arrival time and distance from the target position, (c) attitude angles, and (f) z position (altitude), for the case of using viscous damping forces. In a similar fashion, Fig. 8 shows the graph for the case of using NADFs and Fig. 9 is the graph for the case of combining NADFs and clamping control.

## C. Discussions

From the trajectory on X-Y plane in Figs. 7∼9 (a), it is confirmed that all of the three kinds of controller were able to guide the X4-Flyer to the target point while avoiding obstacles. Furthermore, from the graphs of z-position in Figs. 7∼9 (d), it is confirmed that oscillate was very few and the X4-Flyer was able to move while keeping its altitude constantly. Then, attitude angles $\phi$, $\theta$ and $\psi$, were in the realistic range (from $-3.5$ to $4.5$ deg). Therefore, it is proved that the proposed kinodynamic motion planning can be applied to the X4-Flyer control.

By comparing three types of trajectory on the X-Y plane, the trajectory in the case of using viscous damping forces is most similar to the kinematic trajectory. It is interesting to note that for the case of using NADFs, the X4-Flyer reached the target point with about three times faster than the case of using viscous damping forces (see Fig. 7 (b) and Fig. 8 (b)). This is because the viscous damping forces kept its

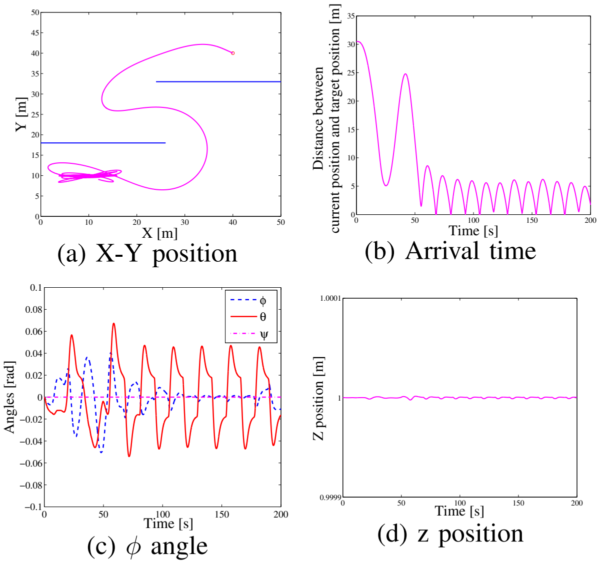


(a) X-Y position (b) Arrival time

(c) $\phi$ angle (d) z position

Fig. 8: Results with NADFs

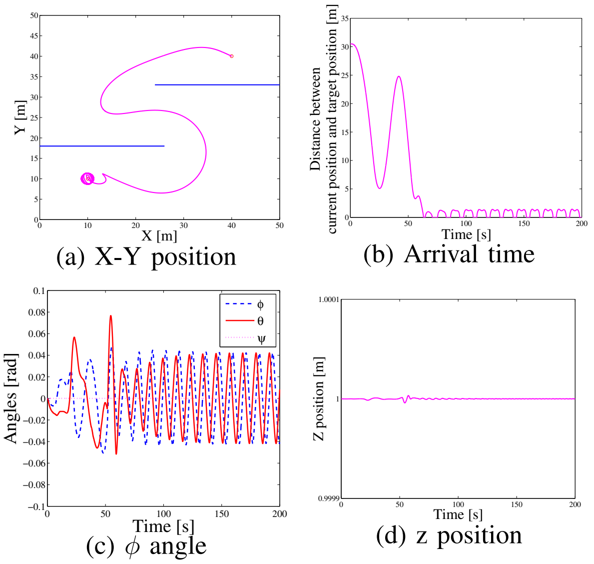


(a) X-Y position (b) Arrival time

(c) $\phi$ angle (d) z position

Fig. 9: Results with combining NADFs and clamping control

trajectory by always suppressing the velocity, but the NADFs can achieve the efficient control by considering the direction of the velocity and suppressing unnecessary forces only.

Note however that for the case of using NADFs, the noticeable oscillation was appeared at around the target point. By applying clamping control, the oscillation was suppressed, but the X4-Flyer was not able to stop on the target point. This is because there is a delay in the controlled response at the attitude control of the X4-Flyer unlike the control of a point mass.

## V. Conclusions

In this research, conventional kinodynamic motion planning for a point mass has been extended to the control of the X4-Flyer. In the proposed method, nonholonomic control and kinodynamic motion planning were combined, and it was confirmed through simulations that the proposed method was able to achieve kinodynamic motion planning for the X4-Flyer. In the simulations, the controller using viscous damping forces and that using the NADFs proposed by Masoud were compared. Then, it was confirmed that the NADFs were able to guide the controlled object more quickly than the case of using viscous damping forces when being applied to the X4-Flyer. Finally, the overshoot was able to be suppressed by applying clamping control.

In future work, the gain optimization is considered by using GA for instance. By optimizing the gains, more efficient control or suppressing of overshoot can be expected. In addition, the experiments using a real machine are considered to evaluate the validity of simulation results.

## References

[1] Y. Nakamura and R. Mukherjee, "Nonholonomic path planning of space robots via a bidirectional approach," *IEEE Trans. on Robotics and Automation*, vol. 7, no. 4, pp. 500–514. Nov. 1991.

[2] JC. Latombe, "Motion planning: A journey of robots, molecules, digital actors, and other artifacts," *Int. J. of Robotics Research*, vol. 18, no. 11, pp. 1119–1128, Nov. 1999.

[3] E. Frazzoli, MA. Dahleh, and E. Feron, "Real-time motion planning for agile autonomous vehicles," *J. of Guidance Control and Dynamics*, vol. 25, no. 1, pp. 116–129, Jan. 2002.

[4] B. Donald, P. Xavier, J. canny, and J. Reif, "Kinodynamic motion planning," *J. of the ACM*, vol. 40, no. 5, pp. 1048–1066, Nov. 1993.

[5] D. Hsu, R. Kindel, JC. Latombe, and S. Rock, "Randomized kinodynamic motion planning with moving obstacles," *Int. J. of Robotics Research*, vol. 21, no. 3, pp. 233–255, Mar. 2002.

[6] E. Rimon and D. Koditschek, "Exact robot navigation using artificial potential functions," *IEEE Trans. on Robotics and Automation*, vol. 8, no. 5, pp. 501–518, Oct. 1992.

[7] J. Peng and S. Akella, "Coordinating multiple robots with kinodynamic constraints along specified paths," *Int. J. of Robotics Research*, vol. 24, no. 4, pp. 295–310, Apr. 2005.

[8] V. Jan, "Navigation of mobile robots using potential fields and computational intelligence means," *Acta Polytechnica Hungarica*, vol. 4, no. 1, pp. 63–74, 2007.

[9] C. Connolly, R. Weiss, and J. Burns, "Path planning using laplace equation," in *Proc. IEEE Int. Conf. Robotics and Automation*, pp. 2102–2106, May. 1990.

[10] I. Tarassenko and A. Blake, "Analogue computation of collision-free paths," in *Proc. IEEE Int. Conf. Robotics and Automation*, pp. 540–545, Apr. 1991.

[11] S. Akishita, S. Kawamura, and K. Hayashi, "New navigation function utilizing hydrodynamic potential for mobile robot," in *Proc. IEEE Int. Workshop Intelligent Motion Control*, pp.413–417, Aug. 1990.

[12] A. Masoud, "Kinodynamic motion planning," *IEEE Robotics & Automation Magazine*, vol. 17, no. 1, pp. 85–99, 2010.

[13] K. Motonaka, K. Watanabe, and S. Maeyama, "Kinodynamic motion planning and control using anisotropic damping forces," in *Proc.* of *Int. Symp. on Artificial Life and Robotics (AROB)*, 2013.

[14] Y. Bouktir, M. Haddad, and T. Chettibi, "Trajectory planning for a quadrotor helicopter," in *Proc.* of *16th Mediterranean Conf. on Control and Automation*, pp. 1258–1263, Jun. 2008.

[15] P. Bristeau, F. Callou, D. Vissiere, and N. Petit, "The navigation and control technology inside the AR.Drone micro UAV," in *Preprints of the 18th IFAC World Congress*, pp. 1477–1484, 2011.

[16] Y. Suh, "Robust control of a quad-rotor aerial vehicle," *Int. J. of Applied Electromagnetics and Mechanics*, vol. 18, pp. 103–114, 2003.

[17] S. Masoud, and A. A. Masoud, "Motion planning in the presence of directional and obstacle avoidance constraints using nonlinear anisotropic, harmonic potential fields: A physical metaphor," *IEEE Trans. on Systems, Man, & Cybernetics, Part A: Systems and Humans*, vol. 32, no. 6, pp. 705–723, Nov. 2002.

[18] B. Samir, M. Pierpaolo and S. Roland, "Design and control of an indoor micro quadrotor," *IEEE Robotics and Automation*, vol. 5, pp. 4393–4398, 2004.